ASSESSING THE ACCURACY OF UAV SURVEYS WITH DIFFERENT CONFIGURATIONS

Ahmed Elaksher[1], David Sanjenis[2], Jose R. Velasco[2], and Mark Lao[2]
[1]College of Engineering, New Mexico State University, Las Cruces, New Mexico, USA, corresponding author, elaksher@nmsu.edu
[2]Cal Poly Pomona University, Pomona, California, USA

KEYWORDS: Photogrammetry, DEM, UAV, Total station, Orthophoto

ABSTRACT:
Recently, developments in airborne sensors and easy-to-fly, reliable, low-cost commercial UAVs have opened a new era for precise aerial mapping. The restricted payload capacity of low-cost UAVs imposes constraints on the quality of their navigation systems and the sensors they can carry. Therefore, the quality of photogrammetric products generated from UAV surveys needs to be assessed. In this study, photogrammetric mapping principles are employed in collecting, processing, and analyzing optical images collected using two UAV surveying systems. The first system was a 3DR Iris+ drone flying at 25 meters above the ground. The second system was a homemade drone similar to Tuffwing flying at about 70 meters above the ground. Both systems carried a Canon PowerShot S100 using a fixed 5.2 focal length. About 30 ground points were surveyed with a TS02 total station and served as the ground truth for data evaluation. After the flights, data was proceeded and geospatial products including DEMs and orthophotos produced were evaluated. Different ground control configurations were examined and ground check-points were used to evaluate the final accuracy of the geospatial products. The comparison of the derived 3D information from captured data with ground measurements showed a high correlation between the accuracy of the 3D products and the sensor specification, flying altitude, as well as image layout. This was supported by comparisons between actual errors and theoretical positional precision based on flying height, photo scale and air base was conducted.

1. INTRODUCTION

Current mapping approaches rely on mainly field surveys or remote sensing techniques. Despite of the high accuracy achievable by ground surveying, they are time-consuming, costly, and unsafe (Thenkabail, 2015). Therefore, alternative technologies that are more cost-effective and of the same or similar accuracy must be investigated. Photogrammetry and remote sensing provide opportunities to gather and interpret qualitative and quantitative information in a more efficient manner. Satellite and traditionally acquired aerial imagery from manned aircraft have been employed in data acquisition systems for a long time (Lillesand et al., 2014). However, these techniques are very costly and they still possess some disadvantages due to their low spatial resolution and limited repeatability (Dandois and Ellis, 2013 and Torres-Sánchez, 2014).

The fast rise of unmanned aerial vehicles (UAVs, i.e., drones) – both military and commercial – has created an opportunity to remotely collect very high-resolution geospatial data for a variety of military and civilian applications (Newcome, 2004). Military applications include terrain analysis, reconnaissance, and battlefield management and damage assessment (Army, 2010). UAVs have also been used intensively in civil infrastructure applications such as post-disaster reconnaissance, geotechnical engineering, and construction management (Greenwood et al. 2019). It has also been used in natural resource management, infrastructure inspection, and precision agriculture (Samad, 2013). Unlike other data collection tools, UAVs can be used in mapping high-risk situations without endangering operators' lives (Nex and Remondino, 2014). They can fly in irregular flight paths to collect essential data without jeopardizing wildlife habitat and species (Christie et al., 2016). In poor weather conditions, they can hover at low altitude to capture data with better quality than that of both aircrafts and satellites images (Xiang et al., 2006). In addition, UAVs are widely utilized in real-time tracking and monitoring moving objects (Rodríguez-Canosa, 2012).

A UAV aerial mapping system includes the measurement platform and all additional hardware and software necessary for flying (Elaksher et al., 2017). They can have fixed or rotary wings, and can fly either remotely via a ground control station or autonomously. In either case, the UAV is equipped with an optical or ranging sensor or a combination of both, a GPS to provide the position and velocity of the UAV, an inertial measurement unit (IMU) to determine its orientation, and an on-board computer to fuse the GPS and IMU observations in real time to navigate the vehicle along a pre-determined flight path (Lee et al., 2016). However, the restricted payload capacity of low-cost UAVs imposes constraints on the quality of their navigation systems and the sensors they can carry (Whitehead and Hugenholtz, 2014). The commonly used sensors are amateur video cameras or consumer grade cameras (Yanagi and Chikatsu 2015), Light Detection And Ranging (LiDAR) sensors with limited sample rate (Carreon-Limones et al., 2017), or small format hyperspectral sensors (Zheng et al., 2016).

Photogrammetric processing of UAV imageries has been investigated in different applications. For example, Gonçalves and Henriques (2015) generated Digital Elevation Models (DEMs) of ten centimeters spacing and about four centimeters vertical accuracy with a Canon Ixus 220 HS flying at a height of 125 meters above the ground and with a Ground Sampling Distance (GSD) of 4.5 cm and a focal length ranging from 4.3 to 21.5 mm. Martínez-Carricondo et al. (2015) reported horizontal accuracy of about three centimeters and vertical accuracy of about five centimeters using a Nikon D-3100 digital reflex camera flying at an altitude of 120m above ground level with a fixed focal length of 16 mm and GSD of three centimeters. Kršák et al. (2016) compared data collected with a TS 02FlexLine total station and a Phantom 2 Vision UAV flying with an altitude of 35 meters above the average height of the terrain. The UAV is equipped with a 14 Megapixels FC200 camera that makes a Ground resolution of one centimeter per

pixel. Results showed that 44% of the points had a deviation of up to five centimeters from the reference surface.

Gillan et al. (2017) compared SfM-generated DTMs to check points surveyed with a Leica TS02 total station. Horizontally the data had a disagreement of about one and half centimeter while a vertical disagreement of about three centimeters was observed. The research was conducted with a Canon EF 35 mm focal lens camera flying at about 150 meters with a GSD of about three centimeters. Zhang and Elaksher (2012) reported half a centimeter discrepancy between data collected with UAVs and onsite manual measurements in mapping road distresses. They flow a Canon EOS Digital Rebel XTi digital camera with a focal length of 50 mm at about 45 meters above the ground.

Recent studies have employed total stations to improve the accuracy of UAV position estimation, Hankus-Kubica et al. (2020); assess the accuracy of the imagery obtained by using a mounted target prism on the UAV, Paraforos et al. (2022); and track UAV position in a non-GNSS environment, Ishii et al. (2020). In addition, Sun et al. (2022) employed a UAV system in displacement measurement. The study showed average errors in the range of one to 40 millimeters in the X and Y directions and average errors in the range of 70 millimeters in the Z direction. In Adi et al. (2023), a UAV system was used for measuring railway ballast profile along a railway alignment. Comparison with total station surveys showed a differences of 0.03 cubic meter for cut volume and 0.13 cubic meter for fill volume.

2. STUDY AREA & DATASET

We conducted this study at the JER Recreational Park north of Las Cruces, New Mexico, USA. The field is located at Latitude: N32° 29' 17.7" and longitude: W106° 42' 56.1" and has an approximate altitude of 1300 meters above the ground. Before we started, we distributed about 40 bucket lids on the ground, Figure 1. Each lid is 12 inches in diameter and has been marked with a 1 inch by 1 inch square of contrast color at the center. The points were surveyed with a Leica TS02 total station. Field procedures, specifications, calibration standards, and recommendations in Ghilani and Wolf (2011) were followed.
Two different flights were conducted with a Canon PowerShot S100 on 24 February 2016. The focal length of the camera was fixed at 5.2 millimeters. The first set of flights was carried out with a 3DR Iris+ drone. The drone was flying at about 25 meters above the ground. A second set of flights was conducted with a homemade drone similar to Tuffwing flying at about 70 meters above ground Figure 2. To estimate the ground coordinates in State Plan Coordinate System (SPCS) and Orthometric heights, we surveyed two extra points via a static GPS survey with Topcon Hiper Lite+.

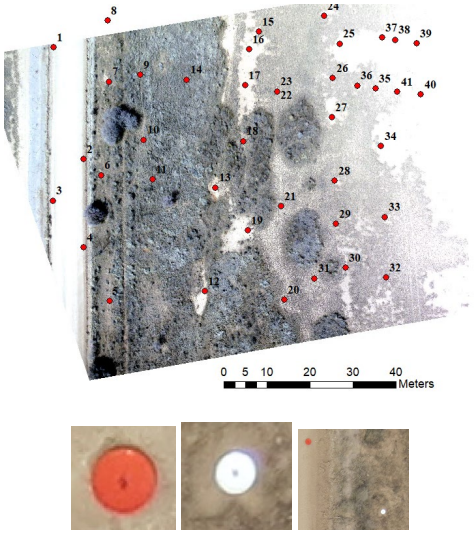

Figure 1 Ground control points used in the experiments

Figure 2. UAV systems used in this study

3. METHODOLOGY

In this section, we present the photogrammetric procedure to process UAV collected images. It starts by camera calibration and then proceeds to relative orientation. Afterward, the relationship between ground and image coordinates is defined using the collinearity equation through ground control points. Finally, high-quality DEMs are generated using automatic image matching and then refine with least squares matching.

3.1. Camera Calibration

Camera calibration is necessary for extracting accurate 3D information from images. The aim of camera calibration is to calculate the so-called inner orientation parameters (focal length, lens distortion, …) this is particularly important for non-metric cameras. We start by calibrating the camera using a self-calibration process with the commercial tool iWitness (Cronk et al., 2006). The software allows for calibrating non-metric cameras and no field or office special arrangement or

preparation is needed. During calibration, black and white targets are randomly distributed on the floor or wall and several images are recorded for the scene. Ten to twelve images are then recorded. Afterward, the calibration is performed automatically, delivering the calibrated focal length, the principle point coordinates and the distortion parameters. Figure 3 shows the estimated calibration parameters for the camera used in this study.

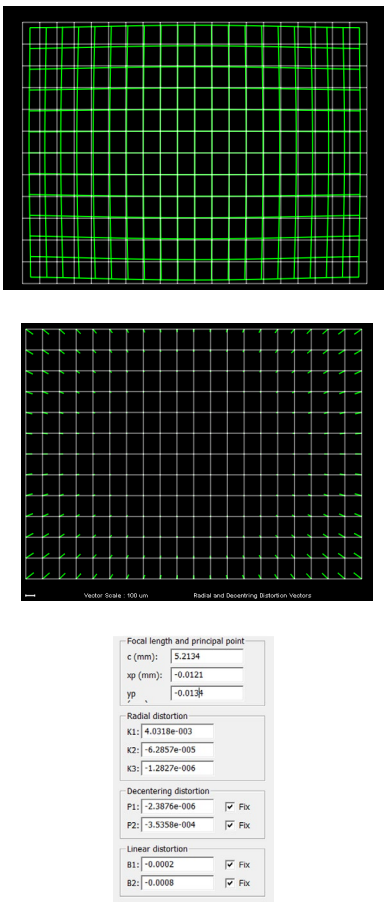

Figure 3. Lens distortion and camera calibration results

3.2. Image Orientation

Several algorithms have been developed to process optical images acquired with cameras carried on UAV mapping systems. These algorithms are based on photogrammetry or Structure from Motion (SfM) concepts used for 3D reconstruction and measurement. In this article, we follow traditional photogrammetric procedures to generate topographic solutions. After the calibration step, the acquired images undergo relative photogrammetric orientation using tie points and absolute photogrammetric orientation using ground control points. This results in precise orientation parameters that allow for the computation of the 3D location of each ground point from the UAV images. Afterward, multiple image matching is conducted to automatically generate three-dimensional surface models and ortho-rectified images.

In relative photogrammetric orientation, images are relatively oriented to each other by identifying and corresponding conjugate points across image pairs. The SIFT algorithm (Lowe, 2004) is used for such task. The SIFT operator is invariant to image transformations: scale, translation, rotation, and skew. First it locates key-points and provides local descriptors for each point. Next, the point descriptors are explored to determine point correspondences among all image pairs. Candidates' matches are identified with the minimum Euclidean distance for the invariant descriptor vector. These points then serve as pass (tie) points to provide geometric strength and make a rigid, and redundant, structure for absolute orientation.

Absolute orientation is next carried out to replicate the precise geometric relationship between ground points and their corresponding image points. Through this process, the camera positional and orientation parameters are estimated through a defining a set of distinct Ground Control Points (GCPs). The locations of the GCPs could be determined before or after the aerial survey using conventional surveying equipment such as total stations or the Global Position System (GPS) depending on the accuracy, size, and characteristics of the pilot site. Approximate positional and orientation parameters are needed for this step and are approximated from the GPS and INS sensors on board of the aerial vehicle. The ground coordinates of pass points are also determined through this step adjustment. Figure 4 is an example of the oriented photos with a generated initial point cloud produced by matching the tie points.

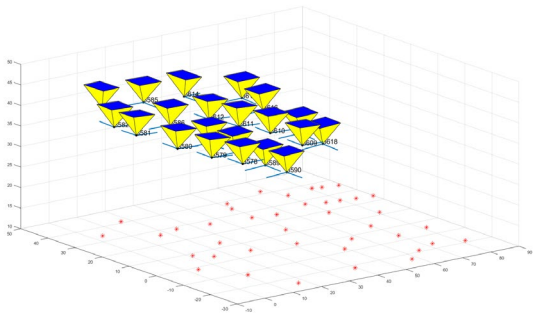

Figure 4. Oriented images in a 3D view

3.3. 3D surface reconstruction

After the orientation is attained, image matching is conducted to automatically generate three-dimensional surface models. There are several matching algorithms developed for generating Digital Elevation Models (DEMs). The first step is always a coarse-to-fine hierarchical strategy as presented in Zhang and Fraser, 2010. Matched key points identified through SIFT are first utilized to reconstruct an initial surface model. Then a distributed ground grid is designed to cover the mapped area with approximate elevations interpolated from the initial surface. Elevations of the grid points are then better estimated by moving the points in the vertical direction and estimating the cross-correlation values between corresponding images. For each elevation, the cross-correlation value is determined and the elevation with the highest value is chosen as the corresponding elevation.

To further improve the matching results, a least square matching model (Elaksher and Bethel, 2010) is then applied. By back-projecting the ground points to the images, pixel intensities will not be equal. In this model, discrepancies among the intensities of corresponding pixels in all images form the observation equations. The unknowns will be the refined heights. Therefore, the observation equations are expressed as functions of the elevations of grid points then the model is to be solved to minimize the discrepancies between the pixels' intensities by moving the grid points vertically. This movement is carried out

in elevation increments corresponding to sub-pixel movement in the image space. The final product is the refined DEM. Figures 5 and 6 exhibit the reconstructed DEMs for one experiment overlaid with the orthophotos for the area. The orthophotos are generated using the refined heights, the values of the image intensities, and camera parameters.

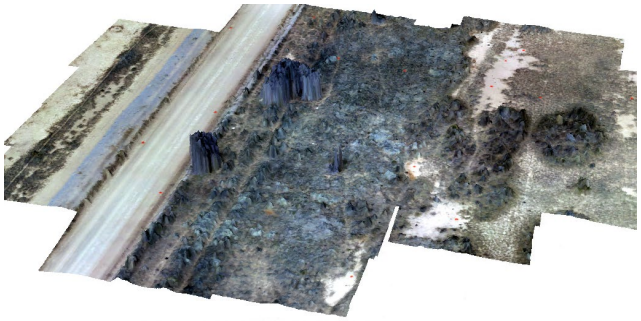

Figure 5. Reconstructed DEM, flying height = 25 meters

Figure 6. Reconstructed DEM, flying height = 70 meters

4. RESULTS AND DISCUSSION

Several experiments were conducted with different configurations of GCPs for each flight. Tables 1 and 2 show the estimated accuracies for check points using different numbers and configurations of GCPs for the 25 meters and 70 meters flying heights.

GCPs	Error in X and Y(cm)		Error in Z (cm)	
	Max	Min	Max	Min
10	2.6	2.4	4.5	4.1
15	2.3	1.8	4.3	4.1
25	2.1	1.9	3.4	2.9

Table 1. Errors in check points, flying height = 25

GCPs	Error in X and Y(cm)		Error in Z (cm)	
	Max	Min	Max	Min
10	5.7	5.4	9.6	8.7
15	3.2	2.8	6.2	5.9
25	3.3	3.1	6.9	5.4

Table 2. Errors in check points, flying height = 70

We can see from tables 1 and 2 that the errors in the horizontal and vertical directions of check points increase as the flying height increases. As the number of GCPs increases, the errors decrease; however, insignificant changes are observed for both experiments. Errors in both the X and Y directions are similar while errors in the vertical direction (Z) are about two times the errors in the horizontal direction (X and Y). The differences between maximum and minimum errors from different configurations are insignificant.

Theoretically, Moffitt and Mikhail (1980) provided a theoretical framework for estimating the positional precision of a ground point. In ideal cases, when the aerial triangulation is error-free, σ_X, σ_Y and σ_Z of ground coordinates can be estimated using:

$$\sigma_X = \sigma_Y = \sigma_p \, . \, S$$
$$\sigma_Z = \sigma_p \, . \, S \, . \, H/Base$$

where H is the flying height, B is the air base of two successive images, S is the photo scale, and σ_p is the parallax accuracy estimated as the square root of twice the standard error of the image coordinates, i.e. σ_i.

The standard error of the image coordinates measurements is a function of the image resolution and the level at which point features can be detected in the images. For most automatic tie point detection algorithms, σi is typically one-third of the camera's physical pixel size. For this study, the estimated σ_X, σ_Y, and σ_Z are 0.7, 0.7, and 1.5 cm respectively for the 25 meters flying height. For the 70 meters flying height, σ_X, σ_Y, and σ_Z are 2, 2, and 5 cm respectively. Because image orientation parameters are not error-free, errors in both the horizontal and vertical directions are bigger than those estimated theoretically. Several experiments were done by excluding different images to assess the effect of change the air base on the accuracy. It was found that the longer the air base the smaller the errors in the check points, which is supported by the theoretical principles.

Conclusion

In this article, we evaluated a low-cost UAV-based aerial surveying system. Low-cost UAVs are flexible systems that are easy to operate and can efficiently capture digital images with very high ground resolution allowing for generating very precise DEMs. Different factors affect the quality of the generated data including flying height, camera characteristics, and distance between successive photos. At higher UAV altitudes, more errors are expected; while the errors decrease as the distance between successive photos increases. GCPS are essential for high quality mapping as the on board GPS and INS systems don't provide surveying-grade positional or orientation data. Therefore, there is an inevitable demand for ground surveys to provide ground control data. This research demonstrates that UAV optical mapping systems can surpass LiDAR, because it can be accurate over different altitudes and also provide an image of the surface's texture.

REFERENCES

Adi, W. T., Aghastya, A., Prihatanto, R., & Agustriana, T. M. (2023, May). Measurement of railway ballast deficiency using UAV drone and total station by graphical, statistical, and volume comparison. In AIP Conference Proceedings (Vol. 2592, No. 1). AIP Publishing.

Army, U. S. (2010). Eyes of the Army. US Army Roadmap for Unmanned Aircraft Systems 2010, 2035.

Carreon-Limones, C., Asher, M., Rashid, A., and Bhandari, S., "3-D Mapping using LIDAR and Autonomous Unmanned Aerial Vehicle," Proceedings of Infotech@Aerospace Conference, Grape Vine, TX, 9-13 Jan. 2017.

Christie, K. S., Gilbert, S. L., Brown, C. L., Hatfield, M., & Hanson, L. (2016). Unmanned aircraft systems in wildlife research: current and future applications of a transformative technology. Frontiers in Ecology and the Environment, 14(5), 241-251.

Dandois, J. P., & Ellis, E. C. (2013). High spatial resolution three-dimensional mapping of vegetation spectral dynamics using computer vision. Remote Sensing of Environment, 136, 259-276.

Elaksher, A. F., Bhandari, S., Carreon-Limones, C. A., & Lauf, R. (2017, August). Potential of UAV lidar systems for geospatial mapping. In Lidar Remote Sensing for Environmental Monitoring 2017 (Vol. 10406, p. 104060L). International Society for Optics and Photonics.

Ghilani, C. D. (2018). Elementary Surveying: An Introduction to Geomatics. Pearson, UK.

Gillan, J., Karl, J., Elaksher, A., & Duniway, M. (2017). Fine-resolution repeat topographic surveying of dryland landscapes using UAS-based structure-from-motion photogrammetry: Assessing accuracy and precision against traditional ground-based erosion measurements. Remote Sensing, 9(5), 437.

Gonçalves, J. A., & Henriques, R. (2015). UAV photogrammetry for topographic monitoring of coastal areas. ISPRS Journal of Photogrammetry and Remote Sensing, 104, 101-111.

Greenwood, W. W., Lynch, J. P., & Zekkos, D. (2019). Applications of UAVs in civil infrastructure. Journal of Infrastructure Systems, 25(2), 04019002.

Hankus-Kubica, A., Brzozowski, B., Cheda, K., Kulinski, M., & Wieczorek, P. (2020, June). Verification tests of total station usability for UAV position measurements. In 2020 IEEE 7th International Workshop on Metrology for AeroSpace (MetroAeroSpace) (pp. 331-335). IEEE.

Ishii, A., Yasuno, T., Amakata, M., Sugawara, H., Fujii, J., & Ozasa, K. (2020). Autonomous UAV flight using the Total Station Navigation System in Non-GNSS Environments. In ISARC. Proceedings of the International Symposium on Automation and Robotics in Construction (Vol. 37, pp. 685-692). IAARC Publications.

Kršák, B., Blišťan, P., Pauliková, A., Puškárová, P., Kovanič, Ľ., Palková, J., & Zelizňaková, V. (2016). Use of low-cost UAV photogrammetry to analyze the accuracy of a digital elevation model in a case study. Measurement, 91, 276-287.

Lee, Y., Yoon, J., Yang, H., Kim, C., & Lee, D. (2016, July). Camera-GPS-IMU sensor fusion for autonomous flying. In 2016 Eighth International Conference on Ubiquitous and Future Networks (ICUFN) (pp. 85-88). IEEE.

Lillesand, T., Kiefer, R. W., & Chipman, J. (2014). Remote sensing and image interpretation. John Wiley & Sons.

Martínez-Carricondo, P., Agüera-Vega, F., Carvajal-Ramírez, F., Mesas-Carrascosa, F. J., García-Ferrer, A., & Pérez-Porras, F. J. (2018). Assessment of UAV-photogrammetric mapping accuracy based on variation of ground control points. International journal of applied earth observation and geoinformation, 72, 1-10.

Moffitt, F. H., Mikhail, E. M., & Photogrammetry, H. (1980). Row. New York.

Newcome, L. R. (2004). Unmanned aviation: a brief history of unmanned aerial vehicles. Publications of the American Institute of Aeronautics and Astronautics.

Nex, F., & Remondino, F. (2014). UAV for 3D mapping applications: a review. Applied Geomatics, 6(1), 1-15.

Paraforos, D. S., Sharipov, G. M., Heiß, A., & Griepentrog, H. W. (2022). Position Accuracy Assessment of a UAV-mounted Sequoia+ Multispectral Camera Using a Robotic Total Station. Agriculture, 12(6), 885.

Rodríguez-Canosa, G. R., Thomas, S., del Cerro, J., Barrientos, A., & MacDonald, B. (2012). A real-time method to detect and track moving objects (DATMO) from unmanned aerial vehicles (UAVs) using a single camera. Remote Sensing, 4(4), 1090-1111.

Samad, A. M., Kamarulzaman, N., Hamdani, M. A., Mastor, T. A., & Hashim, K. A. (2013, August). The potential of Unmanned Aerial Vehicle (UAV) for civilian and mapping application. In System Engineering and Technology (ICSET), 2013 IEEE 3rd International Conference on (pp. 313-318). IEEE.

Sun, J., Peng, B., Wang, C. C., Chen, K., Zhong, B., & Wu, J. (2022). Building displacement measurement and analysis based on UAV images. Automation in Construction, 140, 104367.

Thenkabail, P. S. (2015). Remotely Sensed Data Characterization, Classification, and Accuracies. CRC Press.

Torres-Sánchez et al. (2014) examined discriminating vegetation in wheat fields from images taken by a 12MB Olympus PEN E-PM1 camera fixed on a Microdrone MD4-100 quadcopter.

Whitehead, K., & Hugenholtz, C. H. (2014). Remote sensing of the environment with small unmanned aircraft systems (UASs), part 1: A review of progress and challenges 1. Journal of Unmanned Vehicle Systems, 2(3), 69-85.

Xiang, H., & Tian, L. (2006, July). Development of autonomous unmanned helicopter based agricultural remote sensing system. In ASABE Annual Meeting. Portland, Oregon.

Yanagi, H., & Chikatsu, H. (2015). Camera Calibration in 3d Modelling for UAV Application. The International Archives of Photogrammetry, Remote Sensing and Spatial Information Sciences, 40(4), 223.

Zhang, C., & Elaksher, A. (2012). An Unmanned Aerial Vehicle-Based Imaging System for 3D Measurement of Unpaved Road Surface Distresses 1. Computer-Aided Civil and Infrastructure Engineering, 27(2), 118-129.

Zheng, H., Zhou, X., Cheng, T., Yao, X., Tian, Y., Cao, W., & Zhu, Y. (2016, July). Evaluation of a UAV-based hyperspectral frame camera for monitoring the leaf nitrogen concentration in rice. In Geoscience and Remote Sensing Symposium (IGARSS), 2016 IEEE International (pp. 7350-7353). IEEE.